

Poly Vinyl Alcohol- Based Sol- Gel Synthesis of V₂O₅ Nanoflakes as Positive Electrodes of Li- ion Batteries

Hassan Karami^{1,*}, Asieh Mohammadi²

¹Department of Chemistry, Payamr Noor University, P. O. Box 19395-3697, Tehran, Iran

²Nano Research Laboratory, Department of Chemistry, Payame Noor University, Abhar, Iran

*E-mail: karami_h@yahoo.com

Received: 4 March 2015 / Accepted: 9 July 2015 / Published: 28 July 2015

This work shows a new method to synthesize V₂O₅ nanostructures by poly vinyl alcohol- based sol-gel method. The precursor NH₄VO₃ and polyvinyl alcohol is dissolved in a binary (ethanol/water) solvent to obtain a sol solution and heated until to obtain a homogeneous polymeric gel. During gel pyrolysis in an electrical furnace, vanadium salt is calcined to V₂O₅. The prepared samples are investigated by SEM, TEM, XRD and TGA-DTA. By this method, uniform V₂O₅ nanoflakes with 37 nm average thickness can be synthesized. Electrochemical behaviors of V₂O₅ samples are also investigated in a 0.1M LiClO₄ electrolyte solution prepared in the 1:1 (V/V) ethylene carbonate and dimethyl carbonate solvents by cyclic voltammetry. Finally, some selected V₂O₅ nanomaterials are used as positive electrode materials of Li- ion batteries. The obtained results shows the morphologies and the particles sizes of the cathodic materials can significantly change the redox kinetic rates and charge/discharge performance of the batteries. The Battery made with V₂O₅ nanoflakes shows the highest discharge capacity of 430 mAh g⁻¹ and 280 mAh g⁻¹ for cycles of 1 and 100 at a current density of 100 mA g⁻¹, respectively.

Keywords: V₂O₅ Nanoflakes; Sol-gel; Pyrolysis; Li- ion battery, Positive material

1. INTRODUCTION

Vanadium pentoxide (V₂O₅) crystals is formed in an orthorhombic, weakly bonded layered structure, with vanadium being surrounded by six oxygen atoms forming a strongly distorted octahedron unit [1]. This vanadium compound is the most stable compound in the V–O system, exhibiting highly anisotropic electrical and optical properties due to its orthorhombic structure [2].

Vanadium pentoxide in a layered structure has an energy gap of 2.3eV [3]. V₂O₅ is used in various applications. It has been introduced as a photocatalyst [4], gas sensing agent[5], as well as a

reversible cathode material for lithium batteries [6-8], a window for solar cells [9-10], for electrochromic devices as well as for electronic and optical switches [11-12] and field effect transistors [1]. V_2O_5 nanoparticles have been prepared by a variety of methods such as sol-gel process [14], thermal evaporation [15], reverse micelle [16], hydrothermal [17], vacuum evaporation [18], solvothermal [19] and sputtering [20-21].

The most important application of V_2O_5 is the positive material of lithium ion batteries. Electrochemical reduction of V_2O_5 can occur in a large potential window between 4.0 to 1.5 V vs. Li/Li⁺, where approximately one mole of V_2O_5 is equal to three moles of lithium, leading to a theoretical specific capacity of approximately 442 mAh g⁻¹ [22]. V_2O_5 as positive electrode of rechargeable lithium batteries has low cost, abundant source, high energy density, and high rate charge/discharge towards lithium insertion [23]. In first time, Whittingham has reported the reversible electrochemical lithium intercalation into V_2O_5 at room temperature in 1976 [24]. The inserted lithium value controls phase transitions of $Li_xV_2O_5$. In this series, $Li_xV_2O_5$ is called as α (for $x < 0.01$), ϵ ($0.35 < x < 0.7$), and δ (for $x = 1.0$) phases [25, 26]. For $x \leq 1$, the original V_2O_5 structure can be reformed by delithiation, and all phase transitions are fully reversible [27]. However, for $x > 1$, a partially irreversible transformation is performed from δ -phase to γ -phase [26]. This γ -phase is only reversible in the stoichiometric range $0 < x < 2$ without change to the γ -type structure [25,28]. For $x > 2$, the γ -phase is irreversibly transformed to the ω -phase with a rock-salt type structure. To reach a higher specific capacity and better cyclability, a wide studies has been carried out on modifying the form and the structure of V_2O_5 as positive electrode material depends on its degree of crystallinity, particles sizes and morphology [29-33]. Th previous reports showed that crystalline V_2O_5 has a high specific discharge but has poor cyclability and its crystal structure is damaged by prolonged charge/discharge cycles. Therefore, amorphous and low crystallinity V_2O_5 allows faster lithiation and delithiation [32,33]. Crystal defect during lithiation may be decreased in small crystallites with a high surface area. Therefore, it has higher ionic conductivity. Nevertheless, the recent reports show that the nano crystalline V_2O_5 can change the old concept and acts as high performance positive materials of high discharge rate Li- ion batteries [34-39]

In this project, a new gel network was used to control template-free synthesizing of V_2O_5 nanoflake. The synthesized samples were characterized by scanning electron microscopy (SEM), transmission electron microscopy (TEM), X-ray diffraction (XRD), TGA-DTA and cyclic voltammetry (CV). Finally, the discharge capacity and cyclability of five V_2O_5 nanomaterials with different morphologies and particles sizes were investigated.

2. EXPERIMENTAL

2.1. Material and reagents

NH_4VO_3 , $LiClO_4$, acetonitril, dimethyl carbonate (DMC) and ethylene carbonate (EC) were purchased from Merck. Polyvinyl pyrrolidon (PVP), sodium dodecyle sulfate (SDS), and glycerol were

purchased from Fluka or Aldrich. Carbon black (Super P) was obtained from TIMCAL (Belgium) and poly acrylic acid purchased from Sigma- Aldrich. Double-distilled water was used in all experiments.

2.2. Instrumentals

The morphology of the samples was characterized by scanning electron microscopy (SEM, Philips, XL-30, Netherland), transmission electron microscopy (TEM, Philips, Model EM-208) and X-ray powder diffraction (Philips X'pert diffractometer using Cu [(K α)] radiation with $\lambda = 0.15418$ nm). Cyclic voltammetry (CV) experiments were done by Autolab (Eco Chmie, PGSTAT-10). Thermo gravimetric (TG-DTA) analysis was performed with a PerkinElmer Pyris Diamond, thermal analyzer in air at a heating rate of 10°C/min in the temperature range from 25 to 800°C. All battery experiments were performed by pulse equipped battery analyzer (BTE 05, Karami design group, Iran).

2.3. Synthesis procedure

In this procedure, 91g of a mixed ethanol: water (70:30) solvent was used to dissolve 1g ammonium metavanadate (NH₄VO₃) and 4g PVA. The mixture was heated to 70°C to form a homogeneous sol solution. The obtained sol was slowly heated to evaporate the solvent and form a hard homogeneous polymeric gel. The final gel was pyrolyzed at 560°C for 3 hours. During the pyrolysis process, the PVA polymeric network was slowly burned through the outer surface, and ammonium metavanadate salt was calcinated and converted into V₂O₅ nanoflakes. The obtained samples were crushed to prepare a fine powder. The morphology and particle size of the samples were analyzed by the SEM, TEM, XRD and TG-DTA. The amount of salt, gel-forming agent, solvent composition and synthesis additives were investigated and optimized by the "one at a time" method [40-46].

2.4. Electrochemical studies

In first step, electrochemical behaviors of nanostructured vanadium pentoxide samples synthesized under different conditions were also investigated in a 0.1M LiClO₄ electrolyte solution prepared in the 1:1 (V/V) ethylene carbonate (EC) and dimethyl carbonate (DMC) solvent. The pores of porous graphite electrode were mechanically filled with the synthesized V₂O₅ nanopowder and used as the working electrode in all CV experiments. A platinum electrode and an Ag/AgCl electrode were used as counter and reference electrodes.

In second step, the working electrode was prepared by mixing nanocrystalline V₂O₅ as electroactive materials with 10 wt.% carbon black and 10 wt.% poly acrylic acid (PAA) as binder in ethanol to form a viscous slurry. The slurry of working electrode materials was spread on a thin aluminum foil with dimensions of 5 mm \times 5 mm \times 1 mm, dried, and pressed. The prepared positive electrode included mass loading of 24-5 mg per cm². The prepared working electrode was coupled with two metallic lithium foil with dimensions of 10 mm \times 10 mm \times 1mm as counter and reference

electrodes and immersed in the electrolyte (0.1 M LiClO₄ in a 1:1 v/v mixture of ethylene carbonate (EC) and dimethyl carbonate (DMC)). In all cyclic voltammetry experiments, the electrochemical cell was placed in the argon- filled glow box with oxygen and water content each less than 2 ppm.

2.5. Battery assembling

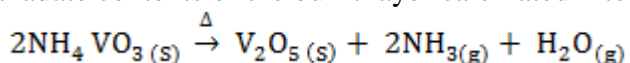
The positive electrode as same with working electrode was prepared by mixing nanocrystalline V₂O₅ as electroactive materials with 10 wt.% carbon black and 10 wt.% poly acrylic acid (PAA) as binder in ethanol to form a viscous slurry. The slurry of cathode materials in ethanol was spread on a thin aluminum foil with dimensions of 20 mm × 20 mm × 1 mm, dried, and pressed. The prepared positive electrode included mass loading of 4-5 mg per cm². Two lithium foil (Aldrich, 99.9%) with dimensions of 20 mm × 20 mm × 1 mm was used as the anodes on both sides of the cathode. Two anode foils, and two glass fiber soaked with battery electrolyte (0.1 M LiClO₄ in a 1:1 v/v mixture of ethylene carbonate (EC) and dimethyl carbonate (DMC)) and one prepared positive electrode were pressed together. After cathode preparing, all processes of battery assembling were done in argon-filled glow box with oxygen and water content each less than 2 ppm. The cells were attached to the battery testing system and cycled at a galvanostatic mode between 2.0 and 4.0 V.

3. RESULTS AND DISCUSSION

Table 1. Experimental conditions of the synthesized samples in optimization set.

NO	NH ₄ VO ₃	% wt PVA	% 1wt Additive	Solvent (V:V)%	Temperature (°C)	Pyrolysis time (h)
1	1	0	-	Ethanol (50) : H ₂ O (50)	560	3
2	1	1	-	Ethanol (50) : H ₂ O (50)	560	3
3	1	2	-	Ethanol (50) : H ₂ O (50)	560	3
4	1	3	-	Ethanol (50) : H ₂ O (50)	560	3
5	1	4	-	Ethanol (50) : H ₂ O (50)	560	3
6	1	5	-	Ethanol (50) : H ₂ O (50)	560	3
7	0.5	4	-	Ethanol (50) : H ₂ O (50)	560	3
8	1	4	-	Ethanol (50) : H ₂ O (50)	560	3
9	1	4	-	Ethanol (50) : H ₂ O (50)	560	3
10	1	4	-	Ethanol (40) : H ₂ O (60)	560	3
11	1	4	-	Ethanol (30) : H ₂ O (70)	560	3
12	1	4	-	Ethanol (20) : H ₂ O (80)	560	3
13	1	4	-	Ethanol (0) : H ₂ O (100)	560	3
14	1	4	PVP	Ethanol (30) : H ₂ O (70)	560	3
15	1	4	SDS	Ethanol (30) : H ₂ O (70)	560	3
16	1	4	glycerol	Ethanol (30) : H ₂ O (70)	560	3
17	1	4	citric acid	Ethanol (30) : H ₂ O (70)	560	3

In this procedure, the gel network rigidity controls the morphology and particles sizes of the synthesized vanadium pentoxide nanostructures. To make uniform V_2O_5 nanoflakes, ammonium metavanadate (NH_4VO_3) molecules were homogeneously dispersed among polymeric network of the gel. Because of get net work rigidity, the dispersed molecules in the gel network cannot alter their position [40]. Therefore, during the pyrrolysis of the gel, outer layers of gel were burn, and ammonium metavanadate contents of the burnt layer calcinated into V_2O_5 . The chemical equation is as follows:



In this method, the amounts of NH_4VO_3 , PVA, solvent composition and synthesis additives were investigated and optimized by the "one at a time" method. Several samples were prepared by changing the synthesis conditions to obtain optimum conditions for synthesizing uniform vanadium pentoxide nanoflakes. Table 1 shows the experimental conditions of the performed synthesizes for optimizing set.

Each sample was characterized by SEM. Based on SEM images and XRD patterns; the amount of each parameter was changed to obtain uniform V_2O_5 nanoflakes.

3.1. Synthesis optimization

The synthesis temperature is an important agent that can affect on the morphology, particle size, and phase composition of the final product. To this end, according to synthesis procedure (section 2.3), a gel sample including uniform dispersed vanadium salt molecules was investigated with the TGA-DTA technique. Figure 1 shows TGA and differential thermal analysis (DTA) curve of V_2O_5 sample.

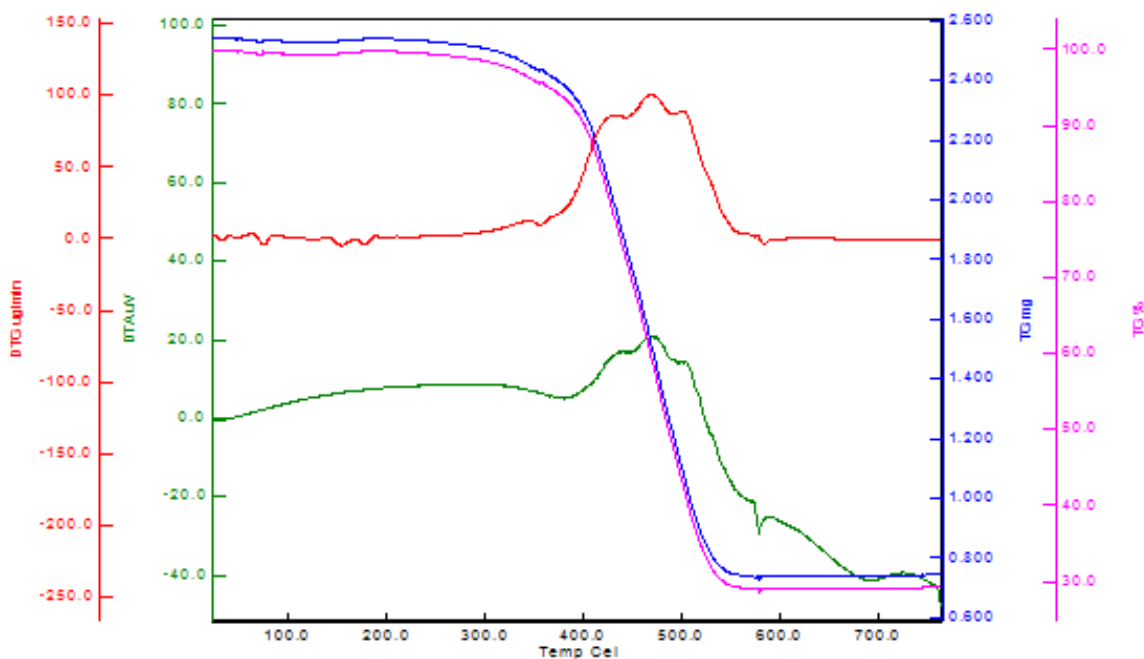
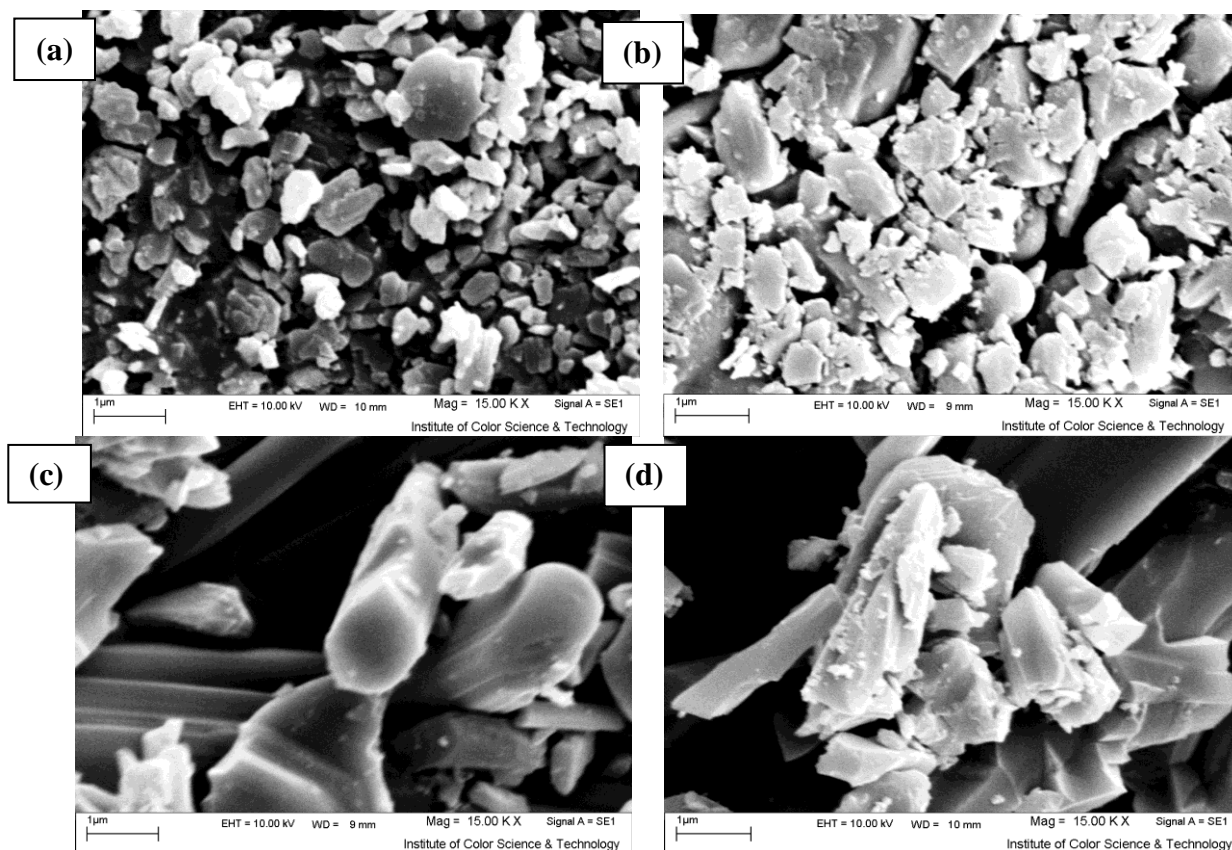


Figure 1. TGA and DTA curves of V_2O_5 sample to determine optimum temperature

The obtained curves shows a slight weight loss between 100-150°C which could be ascribed to the evaporation of the residual solvent, and the main weight loss in the temperatures range of 380–540°C and Inflection point 470°C burning of polyvinyl alcohol (PVA), the decomposition of ammonium metavanadate salt and formation of vanadium pentoxide, respectively. The peak about 580°C is related to the melting of vanadium pentoxide. No weight loss in the range of 540 to 580°C indicates the formation and stability of V₂O₅ as revealed by XRD. Therefore, 560°C is used as pyrolysis temperature in all future experiments.

Experiments 1 to 6 were an optimization set for the PVA as gel making agent. SEM images of the samples were shown in Fig. 2. The nucleation and nuclear growth rates depend on the gel viscosity and rigidity. As it is previously explained [40], the gel specifications such as rigidity and uniformity of the gel are changed by varying PVA, and 4 wt% PVA is an optimum value for V₂O₅ nanoflake synthesis.

Experiments 7 and 8 were used to optimize the weight percentage of ammonium metavanadate in the initial sol. Figure 3 shows SEM images of the synthesized sample in these experiments. As it can be seen Fig. 3, salt percentage can change V₂O₅ morphology from simple spherical nanoparticles to uniform nanoflakes. Vanadium salt amount can control nucleation rate and the particle growth mechanism, but more sample preparing was not possible. Because, the vanadium salt lower than 0.5% wt makes a very small sample which its collection is difficult. A bigger weight percentage of ammonium vanadate was not dissolved in the mixed solvent. Based on SEM images, the sample synthesized of 1%wt has narrower agglomerated nanoflakes, so this value was selected as optimum degree.



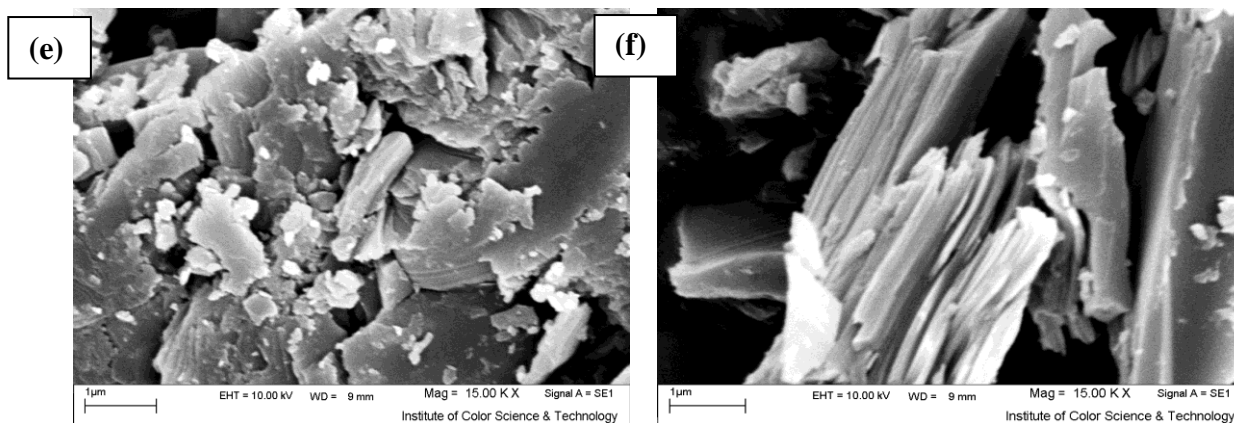


Figure 2. Effects of weight percentages of PVA on SEM images of V₂O₅; (a) 0% wt, (b) 1% wt, (c) 2% wt, (d) 3% wt, (e) 4% wt and (f) 5% wt.

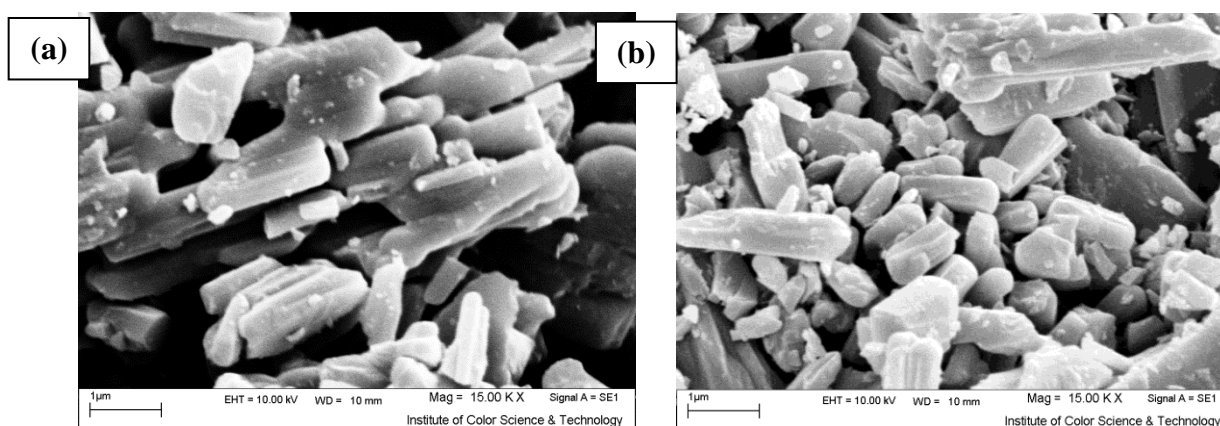


Figure 3. SEM image of V₂O₅ sample synthesized at **a)** 0.5%wt and **b)** 1%wt ammonium metavanadate.

Figure 4 shows the effects of solvent composition on the V₂O₅ morphology and particle size by SEM images (Experiments 9 to 13 in Table 1). As it can be seen in Fig. 4, the composition of mixed solvent controls its polarity and solubility of PVA and salt. When solvent has low water content, it has low polarity so ammonium metavanadate Salt solubility is decreased. At higher volume percentage of water, solubility of PVA is decreased. Therefore, the nucleation and particle growth rates are strongly depends on solvent composition [45]. As an experimental result, the mixed solvent of water: ethanol (70:30) is a suitable solvent to synthesize uniform V₂O₅ nanostructures.

In this work, the effect 1%wt of polyvinyl pyrrolidone (PVP), sodium dodecyl sulfate (SDS), glycerol and citric acid as synthesis additives were studied. Figure 5 shows the SEM images related to the samples prepared according experiments 14 to 17 (Table 1). SDS is an anionic surfactant which can't make an interaction with vanadate anions. In addition, PVP is a polymer which has a long chain including donor sites (nitrogen atoms) to trap vanadate ions. On the other hands, PVP has more solubility in water: ethanol mixed solvent rather than SDS [45].

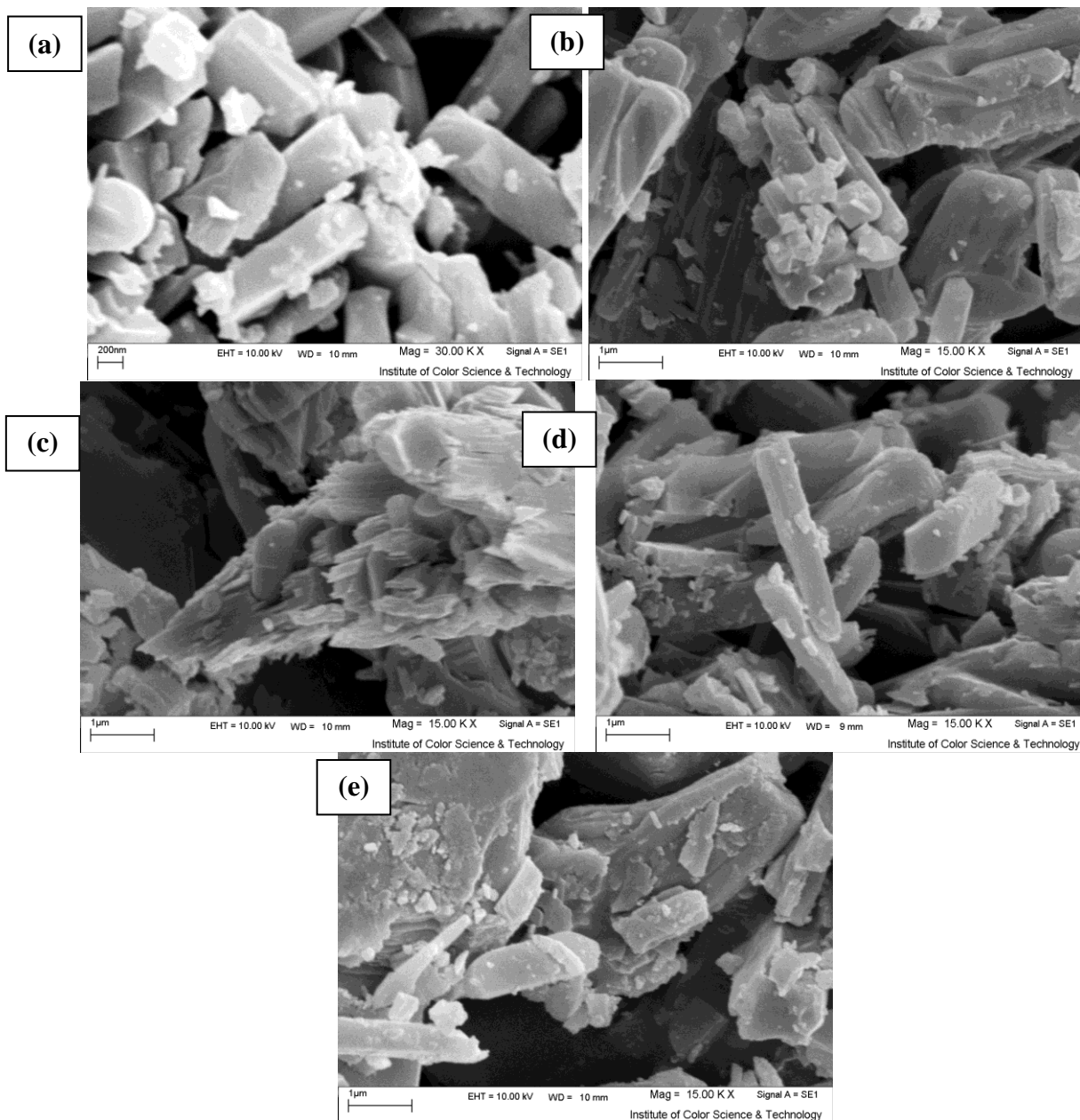
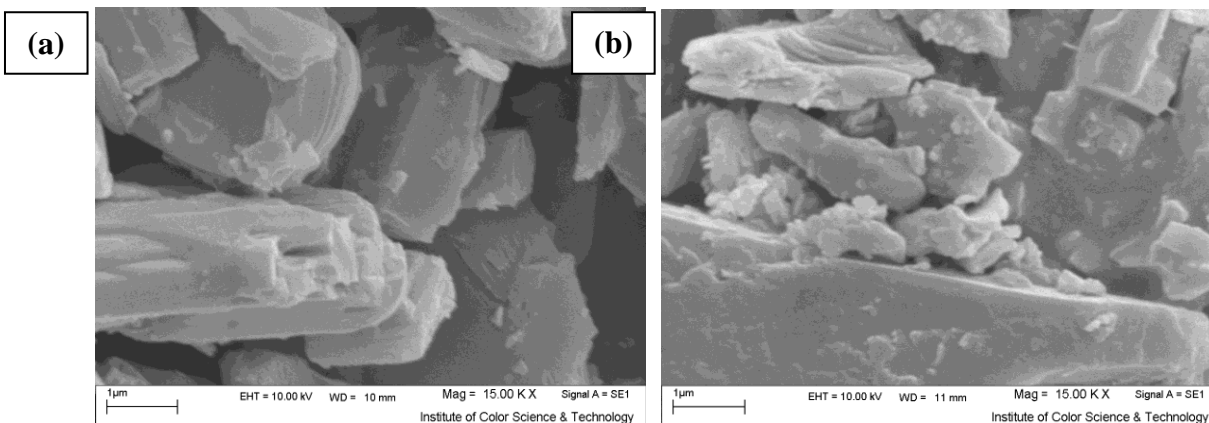


Figure 4. SEM images of samples synthesized at different solvent compositions; (a) ethanol-water (50–50), (b) ethanol-water (40–60), (c) ethanol-water (30–70), (d) ethanol-water (20–80), (e) pure water.



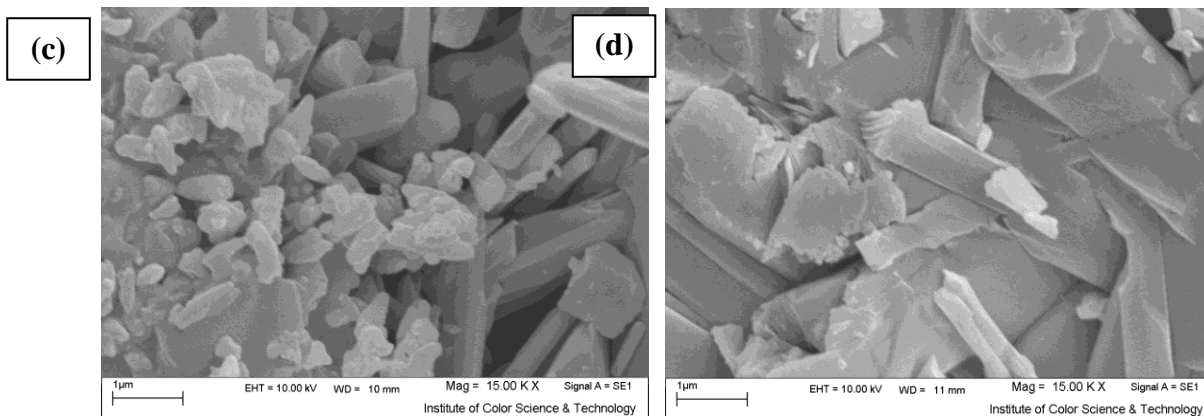


Figure 5. Effect of synthesis additive on the SEM images of V_2O_5 samples; (a) 1% wt citric acid, (b) 1% wt glycerol, (c) 1% wt SDS, (d) 1% wt PVP.

As Fig. 5 shows, 1% wt PVP is a suitable additive to synthesize uniform V_2O_5 nanoflakes. As it can be expected, PVP is a suitable ligand to make an interaction with vanadate ions to control V_2O_5 kinetics and mechanism.

Experiments 1 to 17 showed that the optimum conditions to synthesize uniform nanoflakes are NH_4VO_3 1% wt, PVA4%wt, mixed solvent ethanol-water (30: 70), pyrolysis temperature $560^\circ C$, PVP 1%wt as additive and pyrolysis time 3 h. Based on the SEM and TEM images (shown in Fig. 6), the prepared sample in the mentioned conditions includes flake nanoparticles (V_2O_5) with mean thickness of 37 nm, mean width of 1000 nm and mean length of 5000 nm.

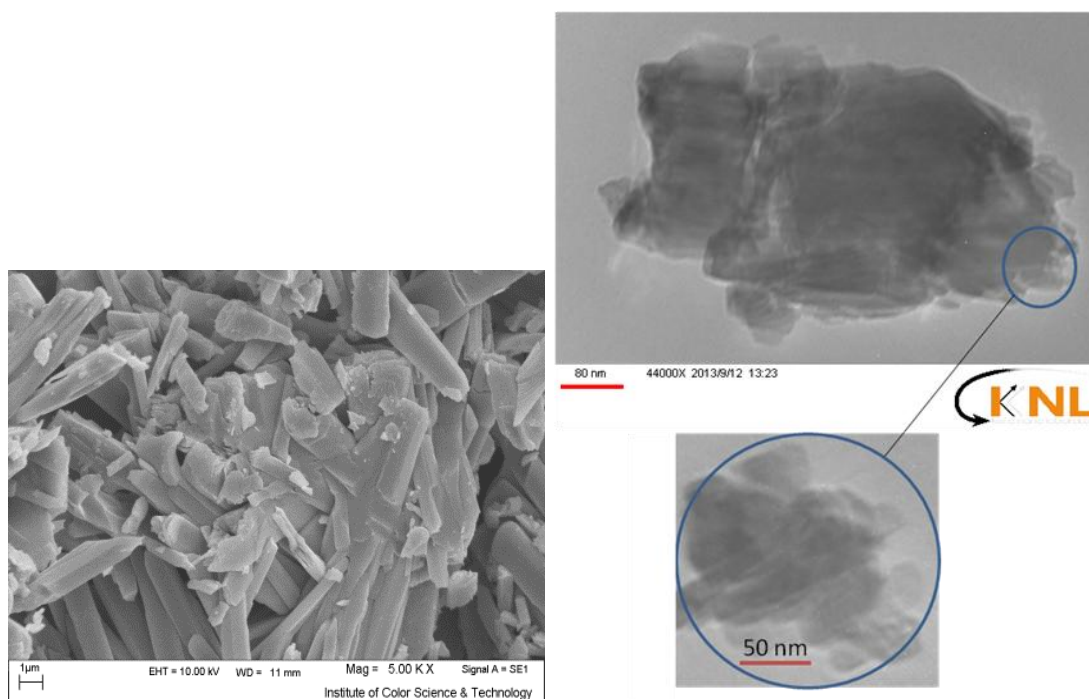


Figure 6. SEM and TEM images of the optimized V_2O_5 nanoflakes.

Figure 7 shows the XRD patterns of the synthesized V_2O_5 sample. As Fig. 7 shows, the sample contains only pure crystalline V_2O_5 (Shcherbinaite) [47,48] as corresponding standard [99-101-2326].

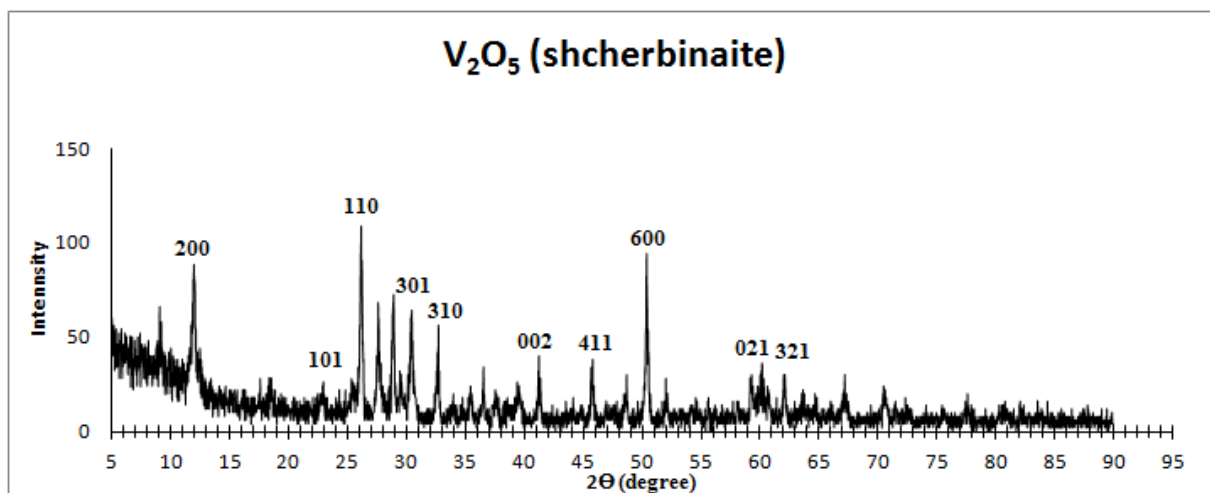
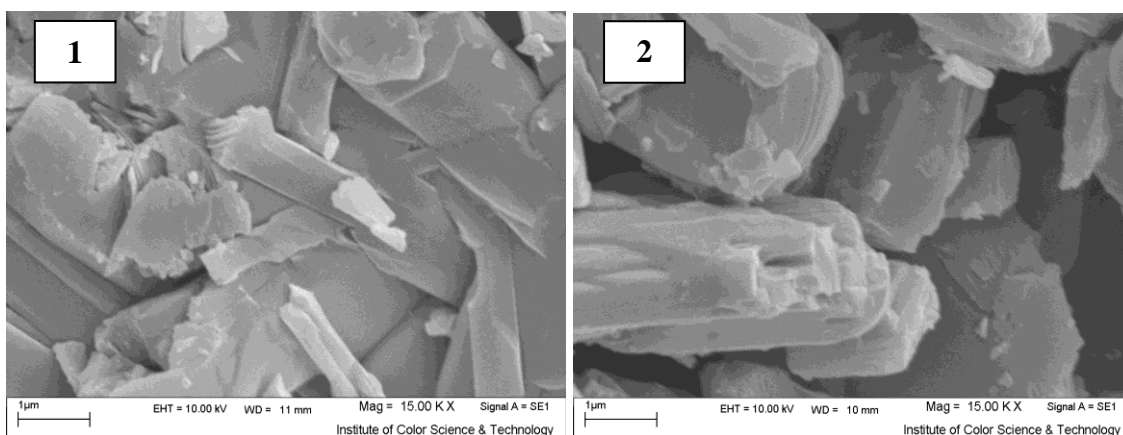


Figure 7. XRD patterns of the nanostructured V_2O_5 sample.

3.2. Electrochemical behaviors of V_2O_5 samples

The electrochemical performance of V_2O_5 samples were studied using cyclic voltammetry with Ag/AgCl reference electrode, Pt counter electrode, and graphite base working electrode. Five nanostructured V_2O_5 samples were synthesized in different synthesis conditions according to Table 2. Figure 8 shows the SEM images of the selected samples for electrochemical studies. Among these samples, sample 5 is selected as a base sample which it doesn't have any synthesis additive. The base sample includes fully crystallized V_2O_5 particles. Sample 1 and sample 2 have been synthesized in the presence of PVP and SDS as suitable structure director additives of V_2O_5 , respectively. This sample includes V_2O_5 nanosheets (nanoflakes). Sample 3 includes non uniform V_2O_5 crystals. The SEM image of sample 2 shows the presence of most agglomerated and non separated V_2O_5 nanosheets. Sample 4 include amorphous V_2O_5 .



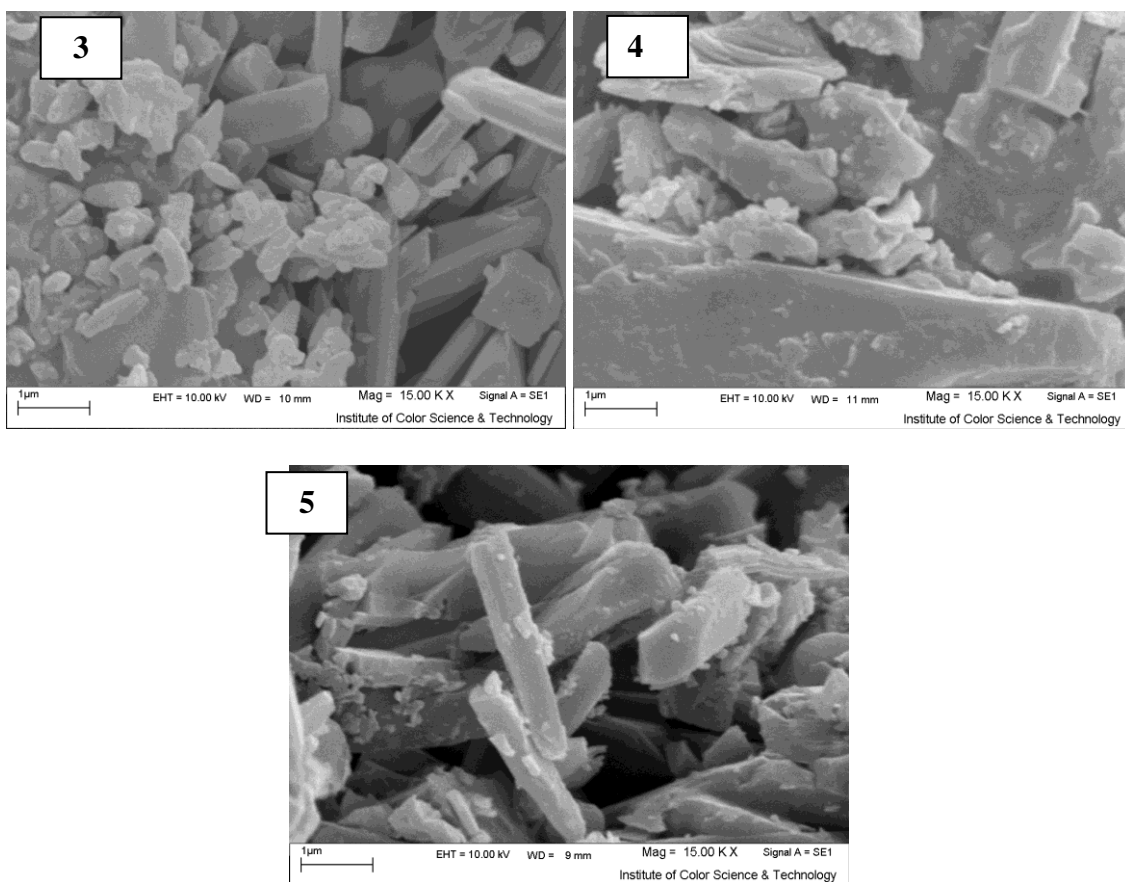


Figure 8. SEM images of nanostructured V_2O_5 samples synthesized in different conditions according to Table 2; Sample 1) in the presence of 1% wt PVP, Sample 2) in the presence of 1% wt citric acid, Sample 3) in the presence of 1% wt SDS, Sample 4) in the presence of 1% wt glycerol, Sample 5) in ethanol: water (20: 80) without additive.

Table 2. Experimental synthesis conditions of five samples (V_2O_5) samples which used in electrochemical studies.

sample	% wt NH_4VO_3	% wt PVA	% 1wt Additive	Solvent (V:V)%	Temperature ($^{\circ}C$)	Pyrrolysis time (h)
1	1	4	PVP	Ethanol (30) : H_2O (70)	560	3
2	1	4	citric acid	Ethanol (30) : H_2O (70)	560	3
3	1	4	SDS	Ethanol (30) : H_2O (70)	560	3
4	1	4	glycerol	Ethanol (30) : H_2O (70)	560	3
5	1	4	no additive	Ethanol (20) : H_2O (80)	560	3

In initial electrochemical experiments, 0.1 M $LiClO_4$ was used as supporting electrolyte in two non aqueous solvents acetonitrile (AC) and 1:1 (V/V) ethylene carbonate (EC) and dimethyl carbonate (DMC). Cyclic voltammograms of the five synthesized V_2O_5 nanostructures with different morphologies and particles sizes were shown in Fig 9. Based on the shown CVs, the mixed solvent of EC/DMC is the better than AC solvent for redox reaction of V_2O_5 samples. In EC/DMC solvent, samples 1 (V_2O_5 nanoflakes) and 5 (fully crystallized V_2O_5) shows the facilitated and faster redox

reactions and more difficult and slow reactions, respectively. However, these tests can not be the basis for a correct conclusion just to compare different V_2O_5 samples.

Based on literature survey results, Watanabe et al used 1 M $LiClO_4$ /butyrolactone as suitable electrolyte for cyclic Voltammetry experiment [49]. There are many reports about the suitability of EC, DMC and EC/DMC mixed solvent as an electrolyte in electrochemical and battery test experiments of V_2O_5 illustrative materials. In a report, Kolytyn et al reviewed some critical aspects related to interactions between cathode materials and electrolyte solutions such as EC, DMC and $LiPF_6$ in lithium-ion batteries [50]. On the other hand, based on the many previous reports such Ref. [51], the metallic lithium electrode is suitable as both reference and counter electrodes in the electrochemical studies of V_2O_5 samples.

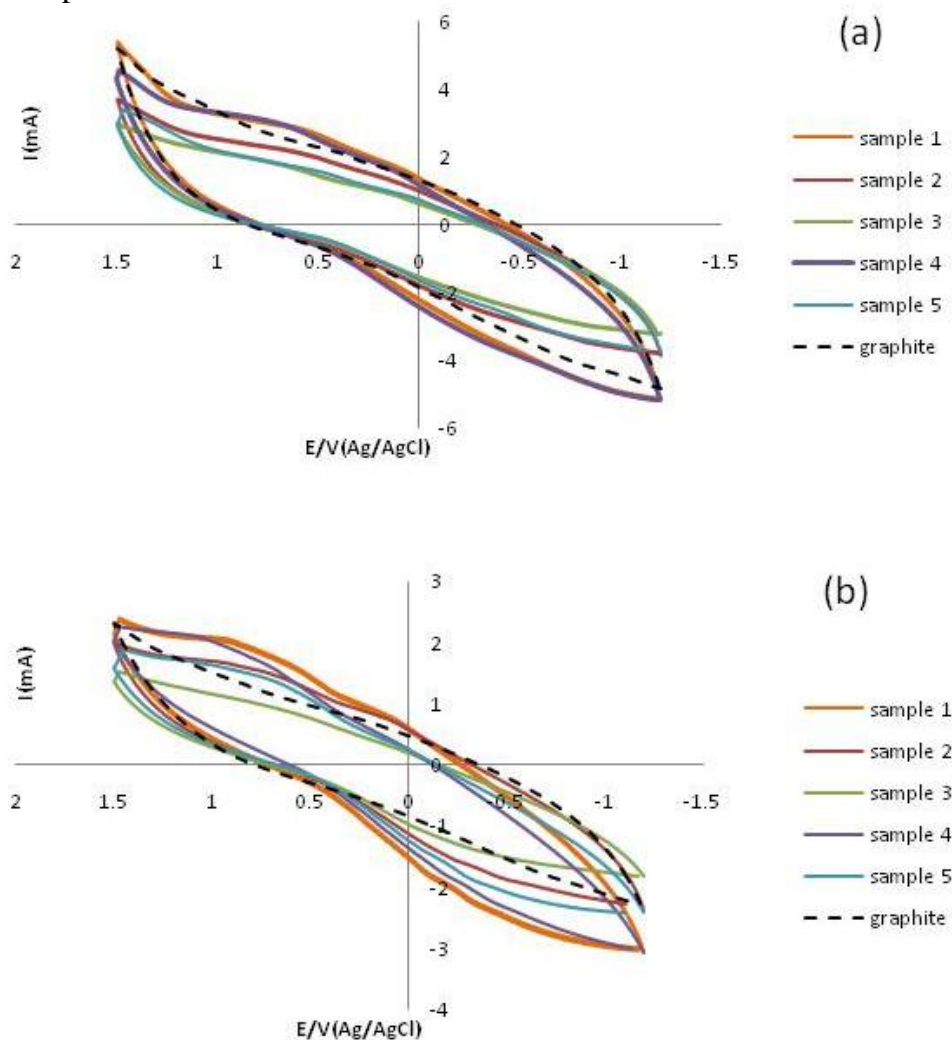


Figure 9. Cyclic voltammograms of graphite electrode filled with V_2O_5 nanoparticles and pure graphite electrode at a scan rate of 100 mV/s in 0.1 M $LiClO_4$ electrolyte; **a)** Acetonitrile, **b)** 1:1 (V/V) ethylene carbonate (EC) and dimethyl carbonate (DMC) solvent.

To improve the redox peaks of V_2O_5 samples, the above mentioned experiments were done by using metallic lithium as counter and reference electrodes. The working electrode is prepared by

mixing the V_2O_5 nanopowders with carbon black, poly acrylic acid as explained in experimental section. The EC:DMC (1:1) mixed solvents include 0.1 M $LiClO_4$ as supporting electrolyte.

Figure 10 shows the second cycles of CV curves of five V_2O_5 electrodes which their synthesis conditions have been shown in Table 2. As it can be seen in Fig. 10, the lithiation and delithiation processes were done in the voltage range of 2.5– 4.2 V vs. Li^+/Li . For the V_2O_5 electrode, during a cathodic scan, two distinct peaks were shown at 3.7–3.6 and 3.3–3.2 V vs. Li^+/Li , which indicated a two steps lithiation process and the corresponding phase was transformed from V_2O_5 to $\epsilon-Li_{0.5}V_2O_5$ (3.37–3.6 V for different samples) and $\epsilon-Li_{0.5}V_2O_5$ to $\delta-LiV_2O_5$ (3.3–3.2 V for different samples). In the following anodic scan, two peaks were also seen at 3.1–3.2 V and 3.5–3.6 V vs. Li^+/Li . The anodic peaks were related to the deintercalation of the lithium ions. In Fig. 10, it is obvious that the exact voltages of anodic and cathodic peaks depend on the sample synthesis conditions. In addition, changes in morphology and particle size of the samples flow to strongly change in the anodic and cathic peak current of both redox couples.

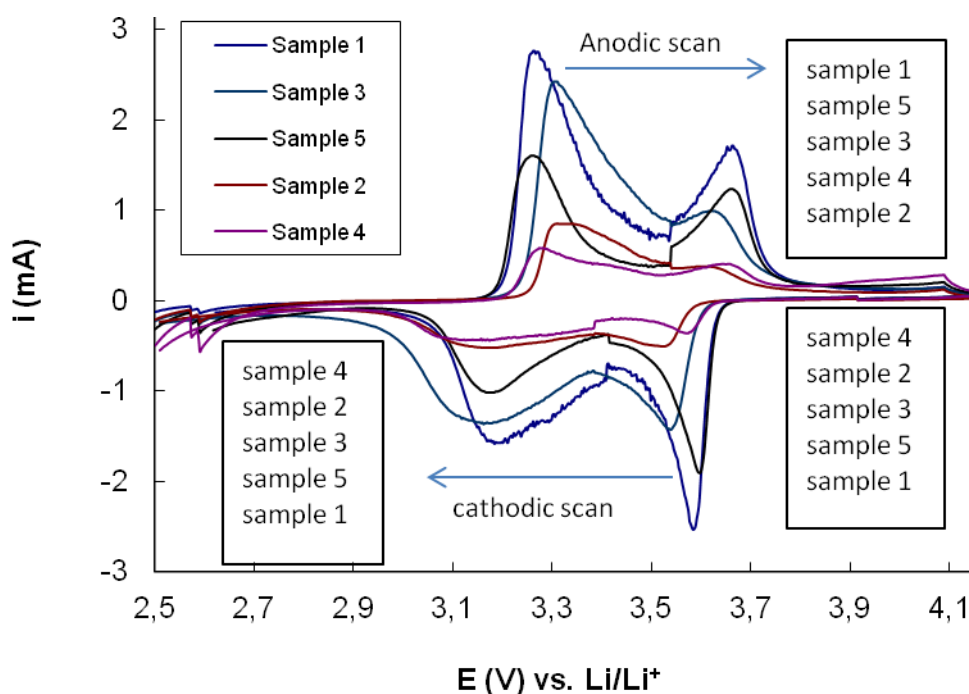
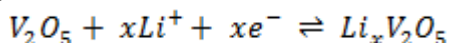


Figure 10. Cyclic voltammograms of five different V_2O_5 samples as working electrode materials versus Li/Li^+ counter and reference electrodes.

Therefore, it can be concluded that the thermodynamic and kinetics of the both redox couple of V_2O_5 depends strongly on the morphology and particle size of the sample. Based on Fig. 10, there are some shifted cathodic and anodic peaks. When a cathodic peak is shifted to the more positive values, the reduction reaction is thermodynamically facilitated. On the other hands, when the anodic peak is shifted to more negative potentials, it shows that the oxidation reaction is facilitated. Sample 1 has

more negative anodic peaks and more positive cathodic peaks because; it includes regular nanoflakes with high effective surface area. Sample 4 is the opposite to the electrochemical behaviors of sample 1. Therefore, it is expected that the V_2O_5 sample contains nanoflakes is the better cathodic material of Li-ion batteries. The potential difference between the positive and negative peaks indicates the polarization of the electrochemical cell. The cell resistance induces cell polarization, which is related to the Li^+ ion transport into and through the positive electrode. This result clearly indicates that the kinetics of lithium deintercalation/intercalation in the V_2O_5 nanoflakes significantly improved by the quick migration of electrons between the V_2O_5 nanoflakes.

The following electrochemical reactions occur in which lithium can be revived on vanadium pentoxide nanoflakes [52]. Electrochemical lithiation occurs together with compensating electrons, leading to the formation of V_2O_5 as follows [53]:



As Fig. 10 shows, in EC: DMC solvent, V_2O_5 samples show relative reversible redox peaks exactly same with those of Li ion/ V_2O_5 rechargeable batteries in charge/ discharge cycles. In both solvents, the peaks currents as kinetic rates are strongly depend on sample morphology and its particle size.

3.3. Battery tests

All samples used in the electrochemical studies, were included in battery tests. In these studies, each V_2O_5 sample was used to prepare a positive electrode for Li-ion battery as it was explained in experimental section. In first step, the discharge capacities of the five batteries constructed with five different V_2O_5 samples (according to Table 2) were determined. Figure 11 shows the first discharge curves of the V_2O_5 based Li-ion batteries at a current density of 100 mA g^{-1} .

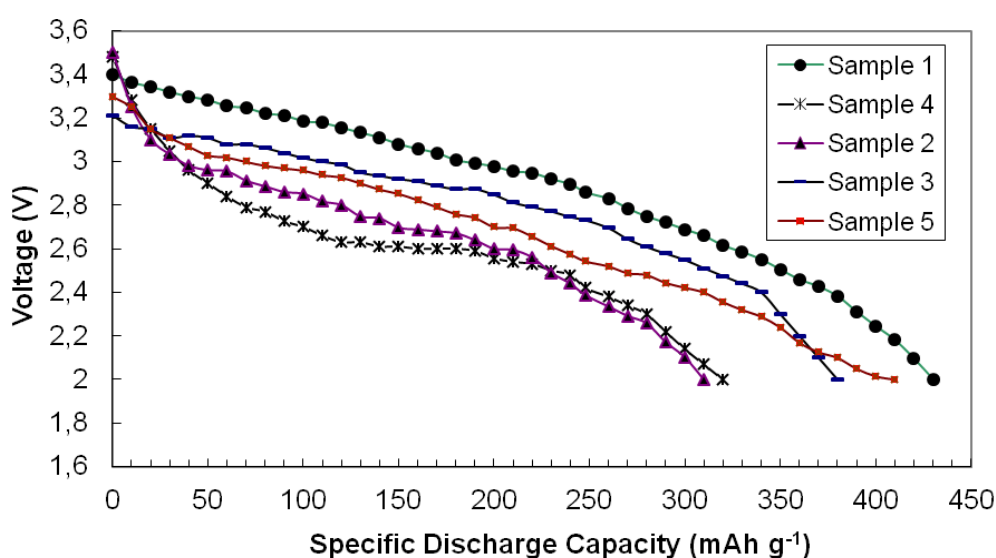


Figure 11. First discharge capacity curves for the five positive electrodes based on V_2O_5 samples (The samples were numbered according table 12).

According to the morphologies of five V₂O₅ samples (Fig. 8), the batteries constructed by V₂O₅ samples 2 and 4 have higher initial voltages than the others. However, during discharge the battery constructed V₂O₅ sample 1 acts better than others. Sample 1 (nanoflakes), sample 5 (regular crystals) and sample 3 (non uniform crystals) are more suitable positive materials of Li- ion batteries. Based on these experiments, the samples 1 to 5 show the first discharge capacities of 430, 310, 380, 320 and 410 mAh g⁻¹, respectively.

To more investigation, the constructed batteries were examined during 100 consecutive charge/discharge processes. Figure 12 shows the consecutive 100 discharge cycles of five Li- ion batteries constructed by the five different V₂O₅ samples.

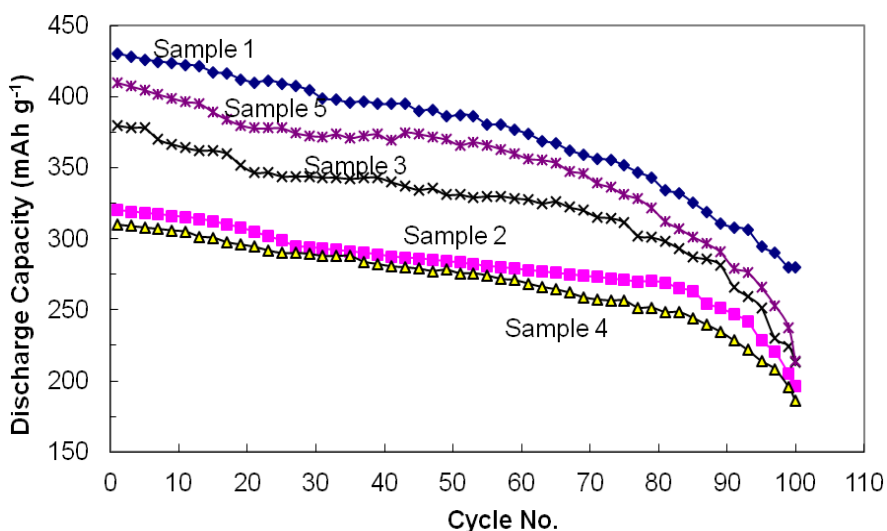


Figure 12. The consecutive discharge curves of the five positive electrodes based on V₂O₅ samples (The samples were numbered according table 12).

As Fig. 12 shows, at cycle 100, discharge capacities of the batteries 1 to 5 are dropped to 280, 185.8, 212.9, 196.5 and 213.7 mAh g⁻¹, respectively. With respect to the first discharge capacities of these batteries, the capacity lose percentages during 100 cycles are calculated as 35%, 40%, 44%, 38.5% and 48%, respectively. Therefore, nanoflakes are the excellent morphology to prepare positive materials of Li- ion batteries. Summary of the obtained discharge data was shown in Table 3.

Table 3. Discharge specifications of five batteries with different cathode materials

Battery No.	Discharge Capacity (mAh g ⁻¹)		Mid Point Voltage (V)	
	Cycle 1	Cycle 100	Cycle 1	Cycle 100
1	430	280	2.86	2.75
2	310	185.8	2.60	2.50
3	380	212.9	2.87	2.67
4	320	196.5	2.70	2.55
5	410	213.7	2.71	2.70

4. CONCLUSIONS

It is concluded that the presented method is a new template-free method based on PVA gel pyrolysis which can be used as a useful and selective method to synthesize pure and uniform V₂O₅ nanoflakes. In this method, the amount of salt, gel-forming agent, solvent composition and synthesis additives are important parameters which can change the morphology and particles sizes of V₂O₅ samples. Many different vanadium pentoxide nanostructures such as spherical nanoparticles and nanoflakes with 37 nm mean thickness can be synthesized by the present method. The cyclic voltammetry results showed that vanadium pentoxide Nanoflakes have areversible half reaction, which can be used as electroactive materials for lithium ion batteries. The battery test results showed that the vanadium pentoxide nanoflakes can be used as excellent cathodic material of Li ion rechargeable batteries with long cyclic life and high discharge capacity.

ACKNOWLEDGEMENTS

We gratefully acknowledge the support of this work by Abhar Payame Noor University (PNU) Research Council. The grant number for support of this work is D-72096-7.

References

1. Y. Zhou, Z. Qiu, M. Lü, A. Zhang, Q. Ma, *Mater. Lett.* 61 (2007) 4073.
2. M. Losurdo, D. Barreca, G. Bruno, E. Tondello, *Thin. Solid. Films.* 384 (2001) 58.
3. W. Yu, J. Wang, Z. Gao, W. Zeng, W. Gao, L. Lin L, *Ceram. Int.* 39 (2013) 2639.
4. J. Wu, Ch. Hsien, *J. Photochem. Photobiol. A.* 163 (2004) 509.
5. S. Zhuiykov, W. Wlodarski, Y. Li, *Sens. Actuators B.* 77 (2001) 484.
6. Y. Wang, G. Cao, *Chem. Mater.* 18 (2006) 2787.
7. C. Julien, H. Poniatowski, C. Loez, M.A. Escobar-Alarcon, J. Jarquin, *Mater. Sci. Eng. B* 65 (1999) 170.
8. R. Lindström, V. Maurice, H. Groult, L. Perrigaud, S. Zanna, C. Cohen, P. Marcus, *Electrochim. Acta.* 51 (2006) 5001.
9. S. Passerini, A.L. Tipton, W.H. Smyrl, *Sol. Energ. Mat. Sol. C.* 39 (1995) 167.
10. A.A. Bahgat, F.A. Ibrahim, M.M. El-Desoky, *Thin. Solid. Films.* 489 (2005) 68.
11. C. Lmawan, H. Steffes, F. Solzbacher, E. Obermeier, *Sens. Actuator B.* 77 (2001) 346.
12. Y. Zhou, Z. Qiu, M. Lü, A. Zhang, Q. Ma, *Mater. Lett.* 61 (2007) 4073.
13. J. Muster, G.T. Kim, V. Krstic, J.G. Park, S. Roth, M. Burghard, *Adv. Mater.* 12 (2000) 420.
14. L. Gao, X. Wang, L. Fei, M. Ji, H. Zhang, T. Shen, K. Yang, *J. Cryst. Growth* 281(2005) 463.
15. C.K. Chan, H. Peng, R.D. Twisten, K. Jarausch, X.F. Zhang, Y. Cui, *Nano Lett.* 7 (2007) 490.
16. C.W. Zou, X.D. Yan, D.A. Patterson, E.A.C. Emanuelsson, J.M. Bian, W. Gao, *Cryst. Eng. Comm.* 12 (2010) 691.
17. D. Pan, Z. Shuyuan, Y.Q. Chen, J.G. Hou, *J. Mater. Res.* 17 (2002) 1981.
18. R.T. Rajendra Kumar, B. Karunagaran, S. Venkatachalam, D. Mangalaraj, S.K. Narayandass, R. Kesavamoorthy, *Mater. Lett.* 57 (2003) 3820.
19. Y. Wang, K. Takahashi, H. Shang, G. Gao, *J. Phys. Chem. B* 109 (2005) 3085.
20. A. Talledo, C.G. Granqvist, *J. Appl. Phys.* 77 (1995) 4655.
21. M. Benmoussa, A. Outzourhit, A. Bennouna, E.L. Ameziane, *Thin. Solid. Films.* 405 (2002) 11.

22. A. Tranchant, R. Messina, J. Perichon, *J. Electroanal. Chem.* 113 (1980) 225.
23. S. Koike, T. Fujieda, T. Sakai, S. Higuchi, *J. Power. Sources* 82 (1999) 581.
24. M.S. Whittingham, *J. Electrochem. Soc.* 123 (1976) 315.
25. J.M. Cocciantelli, J.P. Doumerc, M. Pouchard, M. Broussely, J. Labat, *J. Power. Sources* 34 (1991) 103.
26. J. Galy, *J. Solid. State Chem.* 100 (1992) 229.
27. R.J. Cava, A. Santoro, D.W. Murphy, S.M. Zahurak, R.M. Fleming, P. Marsh, R.S. Roth, *J. Solid. State Chem.* 65 (1986) 63.
28. J. Labat, J.M. Cocciantelli, *French Patent* No. 8916337 (1989).
29. C.J. Patrissi, C.R. Martin, *J. Electrochem. Soc.* 148 (2001) A1247.
30. K.E. Swider-Lyons, C.T. Love, D.R. Rolison, *Solid. State. Ionics.* 152 (2002) 99.
31. A. Singhal, G. Skandan, G. Amatucci, F. Badway, N. Ye, A. Manthiram, H. Ye, J.J. Xu, *J. Power. Sources* 129 (2004) 38.
32. M. Koltypin, V. Pol, A. Gedanken, D. Aurbach, *J. Electrochem. Soc.* 154 (2007) A605.
33. S.H. Ng, S.Y. Chew, J. Wang, D. Wexler, Y. Tournayre, K. Konstantinov, H.K. Liu, *J. Power. Sources.* 174 (2007) 1032.
34. H. Bai, Z. Liu, D. D. Sun, S. H. Chan, *Energy* 76 (2014) 607.
35. V. Varadaraajan, B. C. Satishkumar, J. Nanda, P. Mohanty, *J. Power. Sources* 196 (2011) 10704.
36. Y. Liu, J. Li, Q. Zhang, N. Zhou, E. Uchaker, G. Cao, *Electrochem. Commun.* 13 (2011) 1276.
37. X. Zhang, M. Wu, S. Gao, Y. Xu, X. Cheng, H. Zhao, L. Huo, *Mater. Res. Bull.* 60 (2014) 659.
38. V. Varadaraajan, B. C. Satishkumar, J. Nanda, P. Mohanty, *J. Power. Sources.* 196 (2011) 10704.
39. M. Qin, Q. Liang, A. Pan, S. Liang, Q. Zhang, Y. Tang, X. Tan, *J. Power. Sources.* 268 (2014) 700.
40. H. Karami, A. Aminifar, H. Tavallali, Z.A. Namdar, *J. Clust. Sci.* 21 (2010) 1.
41. H. Karami, M.A. Karimi, S. Haghdar, *Mater. Res. Bull.* 43 (2008) 3054.
42. H. Karami, O. Rostami- Ostadkalayeh, *J. Clust. Sci.* 20 (2009) 587.
43. H. Karami, S. Mmohamadi, *J. Clust. Sci.* 21(2010) 739.
44. H. Karami, E. Mohammadzadeh, *Int. J. Electrochem. Sci.* 5 (2010)1032.
45. H. Karami, E. Fakoori, *J. Nanomaterials* 2011 (2011) 11.
46. H. Karami, A. Rahimi-Nezhad, *Int. J. Electrochem. Sci.* 8 (2013) 8905.
47. D. Habel, O. Goerke, M. Tovar, E. Kondratenko, H. Schubert, *J. Phase. Equilib.* 29 (2008) 482.
48. H. Kaper, M. Willinger, I. Djerdj, S. Gross, M. Antonietti, B. Smarsly, *J. Mater. Chem.* 18 (2008) 5761.
49. H. Watanabe, K. Iton, O. matsumoto, *Thin solid Film.* 386 (2001) 281.
50. M. Koltypin, L. Nazar, B. Ellis, D. Kovacheva, *J. Power Sources* 165 (2007) 491.
51. B. Markovsky, Y. Talyossef, G. Salitra, D. Aurbach, H.-J. Kim, S. Choi, *Electrochem. Commun.* 6 (2004) 821.
52. A. Pan, J. Zang, Z. Nie, G. Cao, B. Arey, G. Li, Sh. Liang, J. Liu, *J. Mater. Chem.* 20 (2010) 9193.
53. Y. Wang, G. Cao, *Adv. Mater.* 20 (2008) 2251.